

## **A 65ka time series from sediment-hosted glasses reveals rapid transitions in ocean ridge magmas**

David J. Ferguson, Yinqi Li, Charles H. Langmuir, Kassandra M. Costa, Jerry F. McManus, Peter Huybers & Suzanne M. Carbotte

### **This file contains:**

- 1. Glass sampling and geochemical analysis**
- 2. Age model and temporal resolution**
- 3. Discussion of temporal versus spatial variation in magma compositions**
- 4. Figures DR1 to DR3**
- 5. Additional references**
- 6. 2017156\_Tables DR1-DR2**

### **1. Glass sampling and geochemical analysis**

Samples of 10 cm<sup>3</sup> of sediment were taken every 1 cm of core length from the base of core AT26-19-12PC upwards. The carbonate portion was removed using a 2N hydrochloric acid leach, after which glass fragments were magnetically separated from the silicate residue. This method yielded hundreds of particles of pristine volcanic glass that were large enough to be analyzed by electron microprobe. Near the base of the sediment the glass comprises a few percent of the sediment mass, then decreases in abundance until only trace amounts are observed in sediments more than ~70 cm above the base of the core. Multiple samples per cm over 70 cm leads to hundreds of samples per core. To overcome the logistical challenges of analyzing so many samples the glass compositions were measured using a Cameca SX Ultrachron electron microprobe at the University of Massachusetts, Amherst, USA. This is a modified microprobe with a high-intensity source and large crystals to maximize count rates, which allowed us to obtain high-precision data for five elements (Mg, Fe, K, Ti and P) during each analysis. We used a beam energy of 15keV, a beam current of 60nA, a 10µm spot size and 60s counting times. The reported compositions for each glass chip are a mean of three analytical spots, providing these had a relative standard deviation of less than a few percent. The data were normalized to the glass standard VE32 using values from Bezos et

al (2009). Two-sigma precision based on replicate analyses of the standard is typically  $\leq 2\%$  for MgO, FeO, K<sub>2</sub>O and TiO<sub>2</sub>, and  $< 10\%$  for P<sub>2</sub>O<sub>5</sub>.

Matrix corrections were made using assumed values for the un-analyzed major elements (e.g. Ca, Al, and Si) typical of those found in mid-ocean ridge basalts (MORBs). The global variations in the concentrations of these elements in MORBs (e.g. Gale et al., 2013) are small enough that this does not represent a significant uncertainty in the reported concentrations for the analyzed elements. For example, varying the assumed Al<sub>2</sub>O<sub>3</sub> content between 14 and 18 wt% translates to a relative change in the calculated FeO and MgO contents of less than 1%. A further simple test of this method is to look at the analytical ‘totals’ when the assumed concentrations are included, which predominantly lie between 99% and 101%.

To provide a test of the accuracy of the Ultrachron data relative to standard electron microprobe analysis (EMPA) we also analyzed a subset of samples via EMPA at the University of Massachusetts Amherst, using the same analytical conditions as Laubier et al (2010). A comparison between 3-analytical spot means from the Ultrachron and 5-analytical spot means from the EMPA, shown in Figure DR1, demonstrates an excellent agreement between the techniques.

## **2. Age model and temporal resolution**

The age and stratigraphy of the host sediments are constrained by Costa et al (2016) using radiocarbon, benthic oxygen isotopes, and stratigraphic correlation of dry bulk density. The oxygen isotope record for the sediment core (shown in Fig 1 in the main paper) generally tracks the benthic global stack (Lisiecki, and Raymo, 2005), with enriched glacial periods ( $> 4.5\text{‰}$ ) and relatively depleted interglacial periods (3.5-4‰). The muted amplitude of glacial-interglacial cycles in  $\delta^{18}\text{O}$  is not uncommon in the North Pacific (e.g. Knudson and Ravelo, 2015). The portion of the core we sampled was deposited during Marine Isotope Stage 15 between ~610-545 ka, a period of ~65 ka. The bottom section of the core that contains glass would have accumulated as the plate moved ~1.8km, well within the likely depositional range for the glasses identified by Clague et

al., (2009). Accumulation rates over this period, shown in Fig. DR2, vary between 0.37-1.6 cm/ka and translate to a nominal temporal resolution of 2.7-0.6 ka per sample. The true temporal resolution, however, may be lower than the nominal resolution due to the smoothing effects of bioturbation, a potential confounding filter on marine records (Berger and Heath, 1968; Guinasso and Schink, 1975; Schiffelbein, 1984). The global average mixing depth is about 10cm (Boudreau, 1994), which would partly smooth the data over 6-27 ka. The effect of bioturbation will be to introduce compositional diversity into the glass population in any one sediment horizon and also to increase the apparent duration of any compositional transitions, making them less distinct. As such the durations of the transitions shown in Figs 4 and DR3 can be considered to be maximum estimates.

### **3. Temporal versus spatial variability in magma compositions**

Although the host sediments have been shown to be in chronostratigraphic order, and therefore the glasses decrease in age from the base upwards, it is possible that an across axis spatial trend in magmatism (i.e. from rift axis to flank) may partly influence the observed chemical variations. It has been argued that lavas erupted on the margins of the neovolcanic zone at Cleft can be more evolved compared to those erupted contemporaneously nearer the axis, the result of a thermally zoned magma lens (Stakes et al., 2006). If a lateral gradient in erupted compositions of this kind existed as a steady state feature, then it is conceivable that the transition from high to low MgO glass reflects the movement of the seafloor through these volcanic zones rather than temporal changes in on-axis compositions. Older on-axis glasses would therefore underlie younger off-axis glasses in the sedimentary record. Although a robust test of any spatial variations in glass accumulation will ultimately require further coring in the vicinity of this core, such a model does not provide a compelling explanation for the data presented here for the following reasons. Firstly, sediments, and therefore glass, can only accumulate once the uppermost lava flow has been emplaced, which is likely to occur near the edge of the neovolcanic zone. If the half-width of the neovolcanic zone is around 2 km then almost all of the sediment that accumulated over the ~65 ka period should contain glass from both magma types, resulting in bi-modal populations. Instead we observe remarkably

constant compositions separated by rapid transitions (Fig 4A-C). Secondly, if more evolved lavas were being erupted at the edge of neovolcanic zone they would re-surface the more mafic flows erupted from the axis, however, the lowermost flow is part of the high MgO trend and matches the composition of the lowermost glasses (marked BC in Figs 4A-C and DR3A-C). Furthermore, a zoned magma lens would likely produce a range of MgO contents between the maximum and minimum observed rather than two distinct populations, and one would expect all of these compositions to be represented in most sediment intervals. Thirdly, a thermally zoned melt lens may account for the different extents of fractionation but cannot produce the distinct  $K_2O/TiO_2$  ratios, which would require a more complex model.

#### 4. Supplementary figures

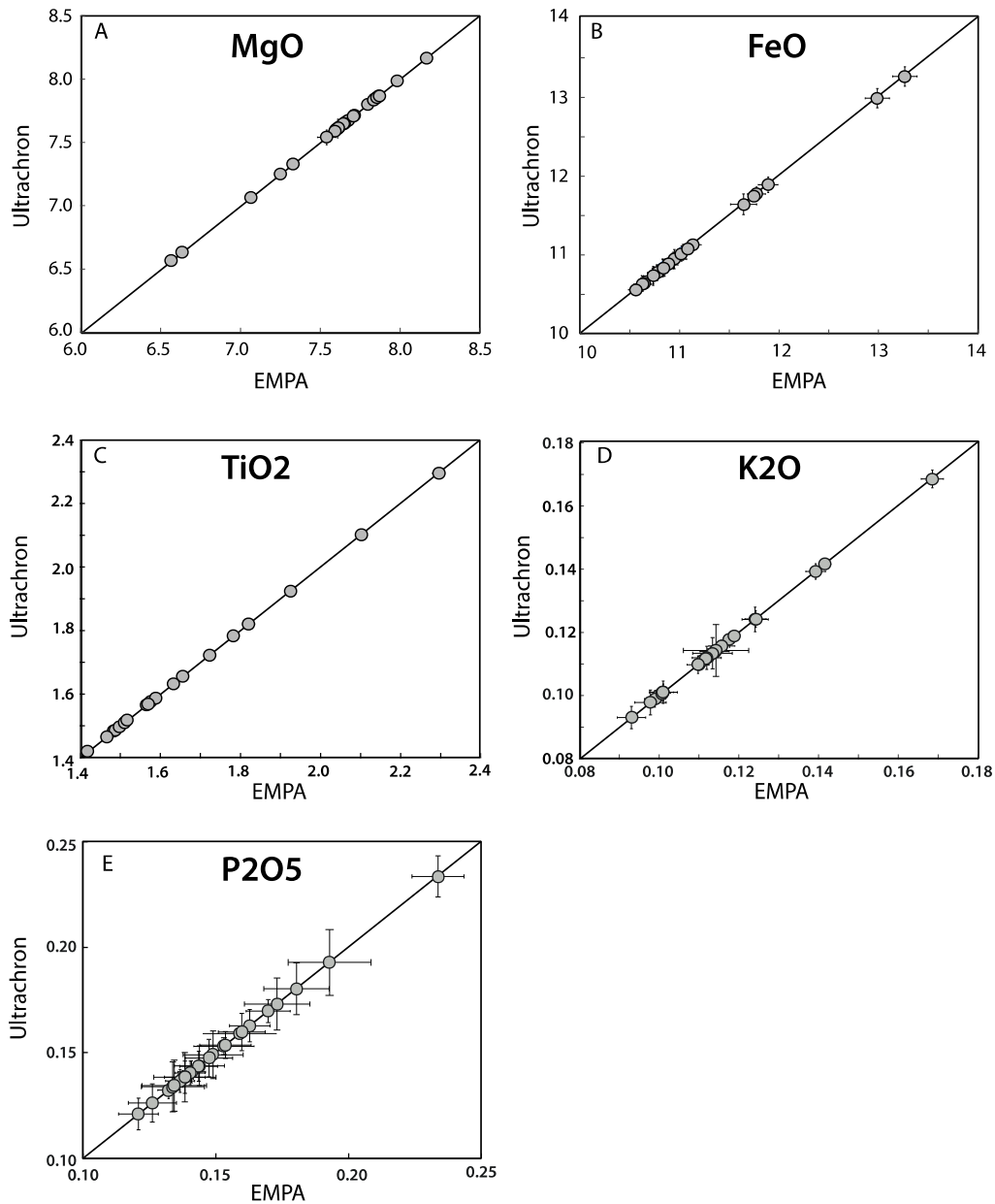


**Figure DR1. Comparison between electron microprobe (EMPA) and Ultrachron data.** Each plot shows the compositions of glass chips from 5-point EMPA means versus 3-point Ultrachron means with 1-sigma uncertainties. Lines show 1:1 correspondence.

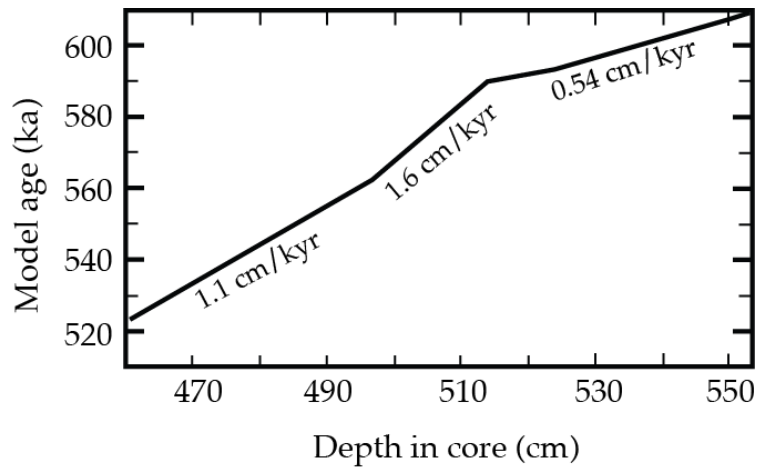


**Figure DR2. Sediment accumulation rates versus age.** Age model and accumulation rates for the section of core AT2619-12PC containing volcanic glass. See Costa et al. (2016) for details

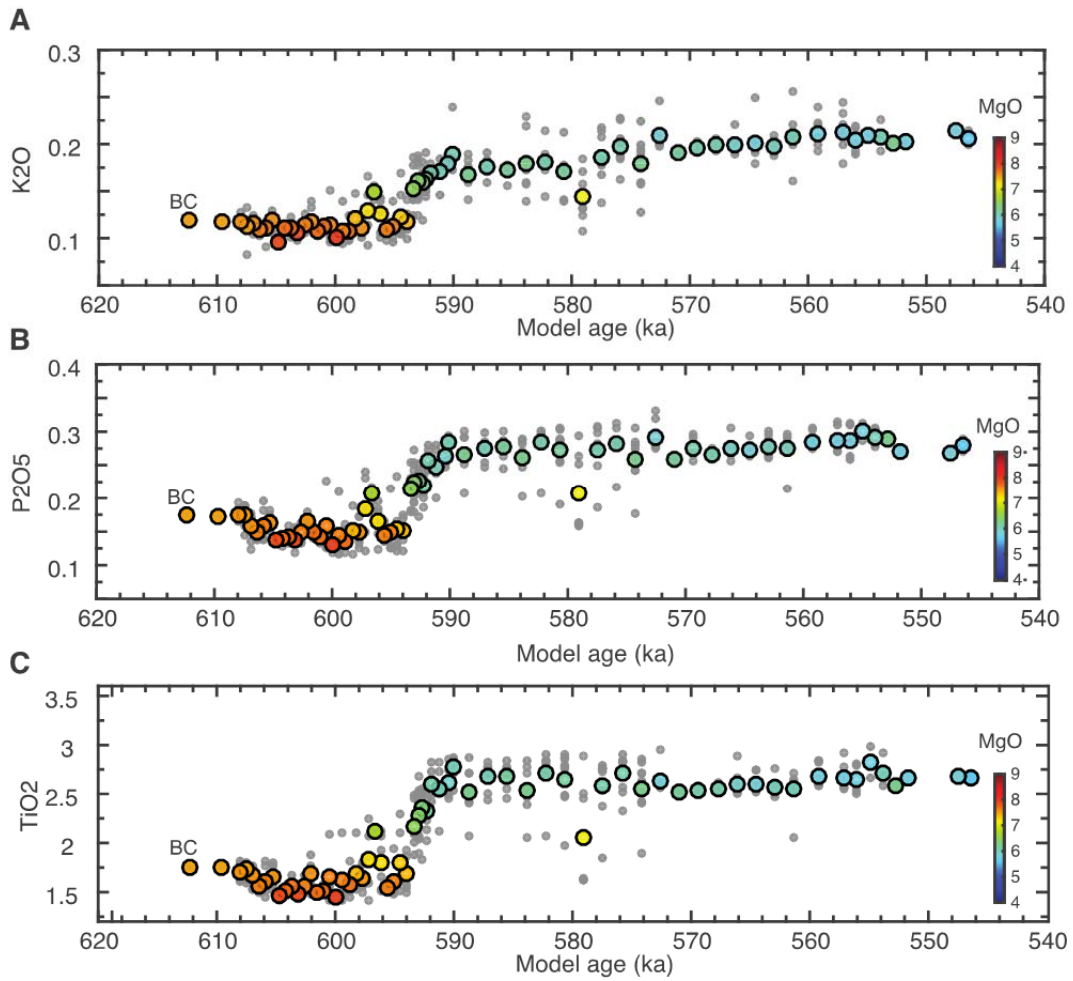


**Figure DR3. A-C** Temporal trends in  $K_2O$ ,  $P_2O_5$  and  $TiO_2$  contents. Similar to  $MgO$  and  $FeO$  (Fig 4A-B) a marked transition occurs in the concentrations of all elements reflecting changing extents of fractional crystallization. Colored symbols show average compositions of glasses per cm of core, grey symbols show individual chips. Points marked 'BC' are from the underlying basaltic crust.

## 5. Additional references

Berger, W. H., and Heath, G. R. 1968, Vertical mixing in pelagic sediments: *Journal of Marine Research*, v. 26, p. 134–143

Bézos, A., Escrig, S., Langmuir, C. H., Michael, P.J. and Asimow, P. D. 2009, Origins of chemical diversity of back-arc basin basalts: A segment-scale study of the Eastern Lau Spreading Center: *Journal of Geophysical Research*, 114, B06212 doi:10.1029/2008JB005924,

Boudreau, B. P. 1994, Is burial velocity a master parameter for bioturbation?: *Geochimica et Cosmochimica Acta*, v. 58, p. 1243–1249

Gale, A., Dalton, C.A., Langmuir, C.H., Su, Y. and Schilling, J.G., 2013. The mean composition of ocean ridge basalts. *Geochemistry, Geophysics, Geosystems*, 14(3), p.489-518.

Guinasso, N.L. and Schink, D.R. 1975, Quantitative estimates of biological mixing rates in abyssal sediments: *Journal of Geophysical Research*. v. 80, p. 3032–3043

Knudson, K.P., and Ravelo, A.C. 2015, North Pacific Intermediate Water circulation enhanced by the closure of the Bering Strait: *Paleoceanography* v. 30, doi:10.1002/2015PA002840.

Laubier, M., Gale, A., & Langmuir, C. H. (2012). Melting and crustal processes at the FAMOUS segment (Mid-Atlantic Ridge): new insights from olivine-hosted melt inclusions from multiple samples. *Journal of Petrology*, egr075.

Lisiecki, L.E., and Raymo, M.E. 2005, A Pliocene-Pleistocene stack of 57 globally distributed benthic  $\delta^{18}\text{O}$  records: *Paleoceanography* 20, PA1003 doi:10.1029/2004PA001071

Schiffelbein, P. 1984, Effect of benthic mixing on the information content of deep-sea stratigraphical signals: *Nature*, v. 311, p. 651–653